

# Hierarchical Self-Assembly of Polyhedral Oligomeric Silsesquioxane End-Capped Stimuli-Responsive Polymer: From Single Micelle to Complex Micelle

Li Ma,<sup>†,§</sup> Haiping Geng,<sup>§</sup> Jiangxuan Song,<sup>§</sup> Jinze Li,<sup>‡,§</sup> Guangxin Chen,<sup>†,§</sup> and Qifang Li<sup>\*,†,§</sup>

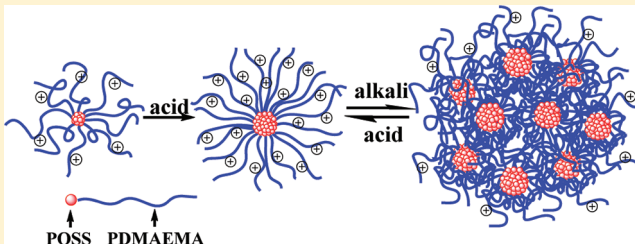
<sup>†</sup>State Key Laboratory of Chemical Resource Engineering, Beijing University of Chemical Technology, Beijing 100029, China

<sup>‡</sup>Key Laboratory on Preparation and Processing of Novel Polymer Materials of Beijing, Beijing 100029, China

<sup>§</sup>College of Material Science and Engineering, Beijing University of Chemical Technology, Beijing 100029, China

Supporting Information

**ABSTRACT:** Responsive polymeric micelles have been widely studied because of their potential use in nanocontainers and nanocarriers. In this study, polyhedral oligomeric silsesquioxane (POSS) end-capped poly[2-(dimethylamino)ethyl methacrylate] (POSS-PDMAEMA), a stimuli-responsive organic–inorganic hybrid polymer, was synthesized via atom transfer radical polymerization (ATRP) using POSS-Br as a macroinitiator. The self-assembly behaviors of POSS-PDMAEMA in aqueous solution were studied by fluorescence probe, transmission electron microscopy (TEM), dynamic light scattering (DLS), high-resolution transmission electron microscopy (HRTEM), and X-ray diffraction (XRD). The results revealed two self-assembly processes of POSS-PDMAEMA. First they self-assembled into a single micelle with the POSS molecules forming a crystal core and the PDMAEMA chains stretching as a corona. Then the single micelles, as building blocks, were able to reversibly form a hierarchical micelle-on-micelle structure (complex micelle) under external stimuli.



## INTRODUCTION

Stimuli-responsive polymers have attracted great interest in recent years because they can be crafted into new smart materials and have unexplored commercial applications.<sup>1–4</sup> Many important substances in living systems are polymers that have the ability to adopt conformations specific to the conditions in their surrounding environment. Similar adaptive behavior is imparted to synthetic polymers, and the stimuli responsiveness is realized by incorporating functional groups that are amenable to a change in character (e.g., charge, polarity, and solvency) along a polymer backbone. The changes of the functional groups cause relatively minor changes in chemical structure, but can be synergistically amplified to bring about dramatic transformations in macroscopic material properties.<sup>3</sup> Usually, stimuli-responsive behavior is easily obtained in polymeric solution because Brownian motion of solvent molecules requires relatively low energies for macromolecular segments to displace solvent molecules;<sup>1</sup> thus, the self-assembly behaviors of stimuli-responsive polymers in solution have been widely studied by varying the surrounding conditions.<sup>5,6</sup> Especially amphiphilic responsive polymers have attracted great interest because of their unique properties of self-assembly into nanoscale aggregates in selective solvents and potential use in nanocontainers and the nanocarrier field.<sup>7–10</sup>

In previous research, the single micelle with a core and a corona has been widely studied. In addition, the micelle-aggregation process has been found when the concentration of the

polymer solution is increased<sup>11</sup> or the polymer structure is designed to be a triblock copolymer with both ends hydrophobic and the middle block hydrophilic.<sup>12–14</sup> However, for the single micelle which has a stimuli-responsive corona, its micelle-aggregation process could be reversibly controlled by external stimuli.<sup>15,16</sup>

Polyhedral oligomeric silsesquioxanes (POSS), a class of unique inorganic components, can be incorporated into polymer chains to produce novel hybrid polymers. A typical POSS molecule, R<sub>8</sub>Si<sub>8</sub>O<sub>12</sub>, has a cubic-shape structure containing an inorganic inner siloxane core (30 Å<sup>3</sup>) with the possibility of chemical modification at each of the eight corners. The incorporation of hydrophobic (hydrophilic) POSS into a hydrophilic (hydrophobic) polymer endows the polymer with amphiphility.<sup>12,13,16–20</sup> Moreover, because POSS molecules have strong aggregating ability, they can effectively control the motion of the chain and induce self-assembled molecular aggregates with controlled nanometer size. Here we synthesized a pH-responsive POSS end-capped polymer, POSS-poly[2-(dimethylamino)ethyl methacrylate] (POSS-PDMAEMA). PDMAEMA, a pH/temperature-responsive polymer,<sup>21,22</sup> is widely studied for its self-assembly behaviors in water<sup>23–38</sup> because of its potential

**Received:** April 23, 2011

**Revised:** August 8, 2011

**Published:** August 09, 2011

use in nanocontainers and nanocarriers.<sup>15,39,40</sup> We found POSS–PDMAEMA experienced two self-assembly processes under external stimuli and at last formed a hierarchical structure; we suggested two self–self assembly mechanisms, i.e., the formation of a single micelle and a complex micelle under external stimuli. First, the single micelle structure with POSS molecules as the core and PDMAEMA as the corona was studied. Then the responsiveness of the complex micelle structure was investigated by varying pH, ionic strength, and temperature.

## ■ EXPERIMENTAL SECTION

**Materials.** Aminopropylisobutyl POSS (apPOSS) was purchased from Hybrid Plastics Co. 2-(Dimethylamino)ethyl methacrylate (DMAEMA; 98%, Alfa Aesar) was dried over calcium hydride ( $\text{CaH}_2$ ) and distilled under reduced pressure immediately before use. 2-Bromoisobutyl bromide (BIBB; 98%, Aldrich), copper(I) chloride ( $\text{CuCl}$ ; 99.999%, Alfa Aesar), and 1,1,4,7,10,10-hexamethyltriethylenetetramine (HMTETA; 97%, J&K Chemical Ltd.) were all used without further purification. Tetrahydrofuran (THF) was distilled from a purple sodium ketyl solution. All other solvents were purchased from Beijing Chemical Reagent Factory and used without further purification.

**Synthesis of POSS–Br Initiator.** THF (10 mL) containing BIBB (0.2759 g, 1.2 mmol) was added to a cold THF solution of apPOSS (0.8745 g, 1 mmol) that contained triethylamine (0.1518 g, 1.5 mmol) at 0 °C. The mixture was magnetically stirred for 1 h at 0 °C and then for another 10 h at room temperature. After filtration, the filtrate was concentrated by a rotary evaporator to yield a product that was a white solid. Then the solid was washed by 5 mL of ethanol and filtrated to obtain the solid. The final product POSS–Br was obtained after vacuum drying with a yield of 70%. <sup>1</sup>H NMR ( $\text{CDCl}_3$ , 500 MHz, ppm): 6.75 (s, 1H,  $-\text{NHCO}-$ ), 3.26 (q, 2H,  $-\text{Si}-\text{CH}_2\text{CH}_2\text{CH}_2-\text{NH}-$ ), 1.96 (s, 6H,  $-\text{C}(\text{CH}_3)_2\text{Br}$ ), 1.85 (m, 7H,  $-\text{Si}-\text{CH}_2\text{CH}(\text{CH}_3)_2$ ), 1.63 (m, 2H,  $-\text{Si}-\text{CH}_2\text{CH}_2\text{CH}_2\text{NH}-$ ), 0.96 (d, 42H,  $-\text{Si}-\text{CH}_2\text{CH}(\text{CH}_3)_2$ ), 0.61 (m, 16H,  $-\text{Si}-\text{CH}_2\text{CH}(\text{CH}_3)_2$ ,  $-\text{Si}-\text{CH}_2\text{CH}_2\text{CH}_2\text{NH}-$ ).

**Synthesis of POSS–PDMAEMA.** POSS–PDMAEMA was synthesized via atom transfer radical polymerization (ATRP) using POSS–Br as an initiator. A typical polymerization procedure was as follows: a 50 mL flask, connected to a standard Schlenk line system with highly pure nitrogen, was charged with POSS–Br (0.3617 g, 0.353 mmol) and  $\text{CuCl}$  (0.0439 g, 0.0353 mmol). Three exhausting–refilling nitrogen cycles were performed to remove oxygen from the system. Then DMAEMA (5 g, 31.8 mmol), HMTETA (0.0977 g, 0.424 mmol), and THF (5 g) were injected into the flask with a syringe, followed by three freeze–evacuate–pump–thaw cycles to remove oxygen from the solution. The flask was sealed under a nitrogen atmosphere and kept in an oil bath at 60 °C. The polymerization was carried out for 3 h and terminated by letting oxygen into the system. The reaction mixture was then allowed to pass through a basic alumina column; the filtrate was concentrated in a rotary evaporator and poured into cold *n*-hexane to precipitate the polymer. Finally, the polymer was dried in a vacuum oven for 12 h.

**Self-Assembly of POSS–PDMAEMA in Aqueous Solution.** All the samples were obtained by directly dissolving the polymers in deionized water. The solutions were stirred at least for 24 h to ensure the system reached equilibrium.

**Characterization.** <sup>1</sup>H NMR measurements were carried out on a Bruker arx-500 spectrometer at room temperature with  $\text{CDCl}_3$  as a solvent and TMS as an internal reference. FT-IR measurements were performed on a Bruker Tensor-27 Fourier transform infrared spectrometer using the KBr disk method. Relative molecular weight and molecular weight distribution of POSS–PDMAEMA were determined with a Waters 515–2410 gel permeation chromatography (GPC) instrument equipped with a Styragel HT6E-HT5-HT3 chromatographic column following a guard column and a differential refractive index detector. The sample solution was filtered with a 0.45  $\mu\text{m}$  syringe filter prior to injection. The measurements were carried out at 35 °C, and THF was used as the eluent at a flow rate of 1.0 mL/min. The system was calibrated with polystyrene standards.

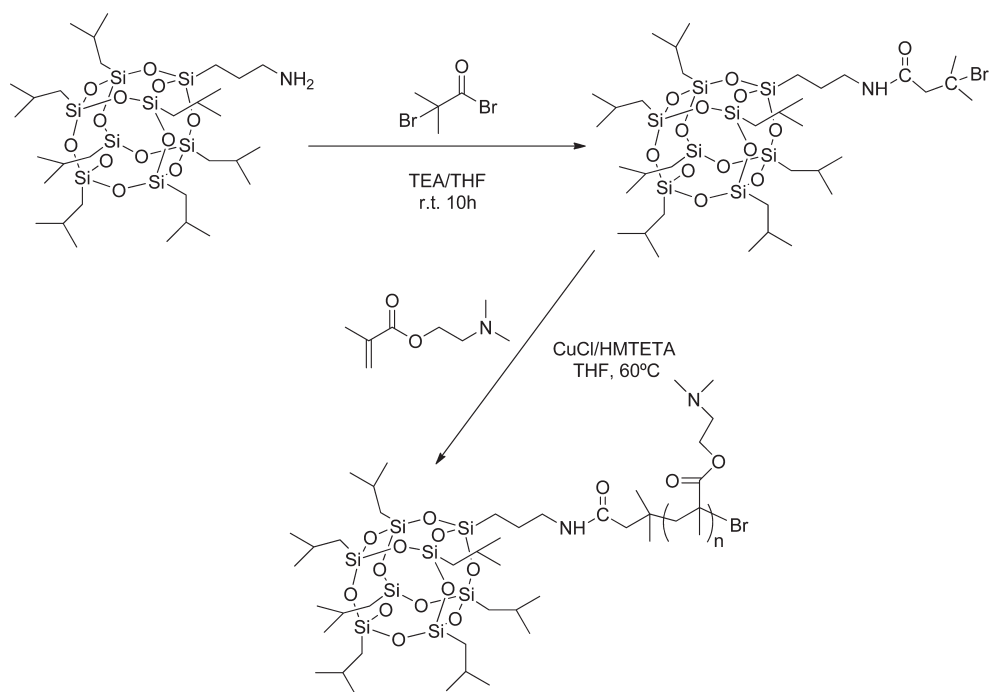
The critical micellization concentration (cmc) was investigated by the fluorescence probe method. Fluorescence spectra were recorded on a Varian Cary Eclipse fluorescence spectrophotometer, and pyrene was used as a hydrophobic fluorescent probe. A predetermined amount of pyrene in acetone was transferred into separate vials, and the acetone was allowed to evaporate. A series of POSS–PDMAEMA aqueous solutions at different concentrations were added to the vials; a final concentration of pyrene was  $6 \times 10^{-7}$  M in each vial. These aqueous solutions were allowed to equilibrate overnight at ambient temperature. Excitation was carried out at 335 nm, and emission spectra were recorded ranging from 350 to 500 nm. The excitation and emission bandwidths were set at 5 and 2 nm, respectively. The ratios of the peak intensities at 384 and 373 nm ( $I_{384}/I_{373}$ ) of the excitation spectra were analyzed as a function of polymer concentration.

Transmission electron microscopy (TEM) images were taken on a Hitachi 800 instrument operated at an accelerating voltage of 200 kV. A drop of 5 mg/mL polymer aqueous solution was directly dropped onto a copper grid (200 mesh) coated with a carbon film, and the sample was allowed to dry at room temperature. High-resolution transmission electron microscopy (HRTEM) images were taken on a JEM 3010 microscope operating at 200 kV, and the samples were made by directly dropping a drop of POSS–PDMAEMA aqueous solution with a specific concentration at different pH values onto a copper grid (200 mesh) coated with a carbon film. X-ray diffraction (XRD) measurements were carried out on a D/max-Ultima III X-ray diffractometer. Scans were taken over the  $2\theta$  range of 3–35° with a scanning rate of 20°/min.

Dynamic light scattering (DLS) measurements were carried out on a Malvern Zetasizer Nano ZS. The measurements were performed at the fixed scattering angle of 90° at room temperature. All samples had a concentration of 5 mg/mL and were filtered using a 0.45  $\mu\text{m}$  Millipore filter before experiments.

## ■ RESULTS AND DISCUSSION

**Synthesis of POSS–PDMAEMA.** The synthetic route is outlined in Scheme 1. The stimuli-responsive POSS–PDMAEMA polymer was prepared by atom transfer radical polymerization (ATRP) from a POSS–Br initiator. The POSS–Br was characterized by <sup>1</sup>H NMR (see Experimental Section) and FT-IR spectroscopy (Figure S1 in the Supporting Information). GPC results showed that the number-average molecular weight ( $M_n$ ) of POSS–PDMAEMA was  $1.85 \times 10^4$  g/mol with a polydispersity index (PDI) value of 1.23; the actual molar ratio of

**Scheme 1.** Synthetic Route of POSS-PDMAEMA

DMAEMA to POSS-Br was 101:1, as determined by <sup>1</sup>H NMR (Figure S2 in the Supporting Information).

**Single Micelle Structure of POSS-PDMAEMA.** The critical micellization concentration (cmc) value is an important parameter for studying self-assembling behaviors; above the cmc value, amphiphilic molecules will aggregate. We used the fluorescence probe method to determine the cmc value of POSS-PDMAEMA. Pyrene is a common probe used to monitor micropolarity because the intensity ratio of the third to the first vibronic peaks ( $I_3/I_1$ ) in the pyrene fluorescence spectrum is sensitive to the polarity; the  $I_3/I_1$  ratio becomes larger in less polar media.<sup>41</sup> The intensity ratio  $I_3/I_1$  versus  $\log C$  ( $C$  is the concentration of POSS-PDMAEMA aqueous solution) is shown in Figure 1, and the cmc value of POSS-PDMAEMA in aqueous solution was determined to be about 0.22 mg/mL.

The formation of a single micelle of POSS-PDMAEMA depended on the cmc value. When the concentration of POSS-PDMAEMA aqueous solution was below the cmc value, POSS-PDMAEMA existed in the form of unimers. We observed the unimers when the pH of the polymer solution was adjusted to 9 (Figure 2a). The size of the small dark dots is ca. 1.0–1.8 nm. The dot cannot contain two or more POSS-PDMAEMA molecules for the following two reasons: First, the Connolly solvent excluded volume of apPOSS calculated by ChemBio 3D Ultra 12.0 was 0.85 nm<sup>3</sup>. Second, the solvent excluded volume of PDMAEMA block should be much larger than that of apPOSS because the molar ratio of DMAEMA to POSS-Br was 101:1. Besides, the PDMAEMA chain became partially hydrophobic when the pH value of POSS-PDMAEMA aqueous solution was 9. Thus we inferred that the PDMAEMA chain precipitated and intertwined around the POSS molecule (Scheme 2C), forming single POSS-PDMAEMA dots in Figure 2a.

When the concentration of POSS-PDMAEMA aqueous solution was above the cmc value, POSS-PDMAEMA self-assembled

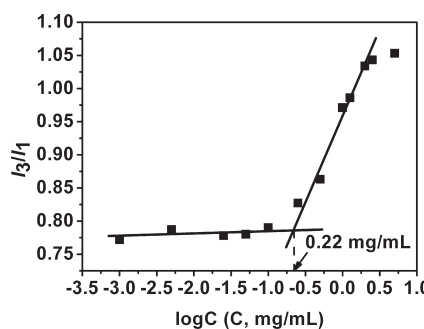


**Figure 1.** Intensity ratio ( $I_{384}/I_{373}$ ) as a function of concentration of POSS-PDMAEMA.

into single micelle structure with POSS molecules as the core and PDMAEMA chains as the corona (Figure 2b). The pH value of POSS-PDMAEMA aqueous solution was adjusted to 3 to make the polymer chain fully extending in water. The size of the dots in Figure 2b is ca. 3–5 nm. These dots only show the core of the micelles, and we cannot see the corona in HRTEM images because PDMAEMA chains were hydrophilic and stretching in low pH aqueous solution.

POSS-PDMAEMA aggregated into micelles not only because it possessed a hydrophobic POSS head and a hydrophilic PDMAEMA block, but also because POSS molecules had strong crystallizing ability (Figure 3a). Figure 2c is a magnified image of a dot in Figure 2b; lattice fringes are observed. Figure 2d shows the electron diffraction pattern of an area in Figure 2b; two diffuse rings and bright short arcs on the rings are observed. From the two images, we can see that POSS molecules formed crystal cores; these crystal cores scattered in the amorphous PDMAEMA chains, forming the pattern in Figure 2d. However, the introduction of the hydrophilic PDMAEMA block

decreased the crystallizing ability of the POSS molecules, as shown in Figure 3.

**Complex Micelle-on-Micelle Structure of POSS–PDMAEMA.** POSS–PDMAEMA possesses pH-responsive property because the PDMAEMA chains can be protonized in acidic aqueous solution. In this study, the effect of pH variation on the self-assembly structure of POSS–PDMAEMA was investigated. POSS–PDMAEMA was directly dissolved in deionized water,

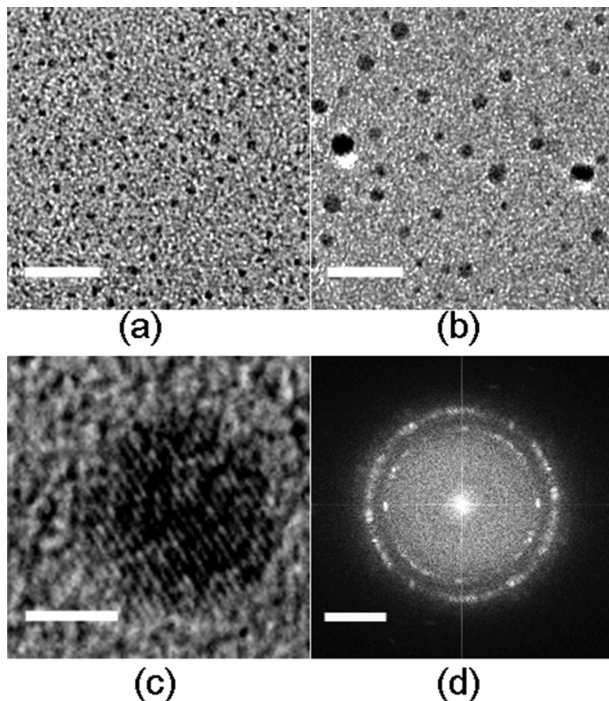
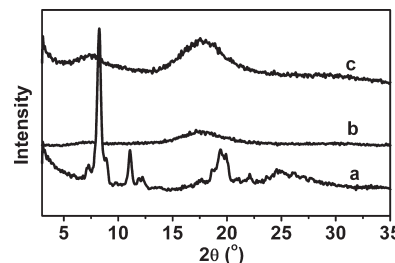


**Figure 2.** HRTEM images of (a) POSS–PDMAEMA unimers obtained from 0.2 mg/mL POSS–PDMAEMA aqueous solution at pH 9.0, bar = 30 nm; (b) POSS–PDMAEMA aggregates obtained from 5 mg/mL POSS–PDMAEMA aqueous solution at pH 3.0, bar = 30 nm; and (c) magnification of (b), bar = 2 nm. (d) Electron diffraction pattern of an area in (b), bar = 6 nm.

and the pH value of the solution was adjusted by 1 M HCl and 1 M NaOH.

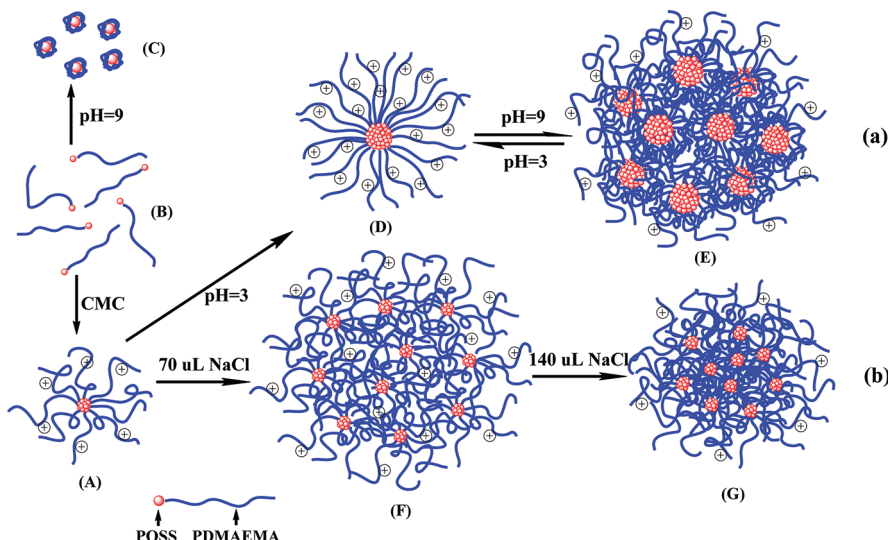
Figure 4 shows that the self-assembly structure of POSS–PDMAEMA was tuned reversibly by varying the pH value of POSS–PDMAEMA aqueous solution. The pH value was first adjusted to 3 (Figure 4a) then to 9 (Figure 4b,c). At low pH aqueous solution, the PDMAEMA chains protonized; thus they were hydrophilic and stretching in the solution, and the POSS heads aggregated to form a crystal core with a size of ca. 3–5 nm, as mentioned above. When the pH value increased from 3 to 9, the PDMAEMA chains gradually deprotonized and became insoluble. This change led PDMAEMA to precipitate around the crystal POSS core, and the simple micelles aggregated into complex micelles (Figure 4b). The aggregates are well-dispersed, and the size is ca. 20–60 nm. Inside the complex micelles, multicompartiment structure can be seen (Figure 4c). Multicompartiment micelles, as a potential delivery vehicle, have been already reported by several researchers; these micelles can keep different medicines separate within the dividing core compartments.<sup>42,43</sup> Finally, the pH value was adjusted back to 3, and the multicompartiment micelles changed back to the small black dots with the size of ca. 3–5 nm (Figure 4d). The experiments summarized in Figure 4 showed that POSS–PDMAEMA had a good pH-responsive property, and its aggregate structure can be controlled reversibly.

The self-assembly aggregate solutions in Figure 4 were also measured by dynamic light scattering (DLS). As shown in



**Figure 3.** XRD spectra of (a) apPOSS, (b) pure PDMAEMA, and (c) POSS–PDMAEMA.

#### Scheme 2. Self-Assembly Process of POSS–PDMAEMA in Aqueous Solution



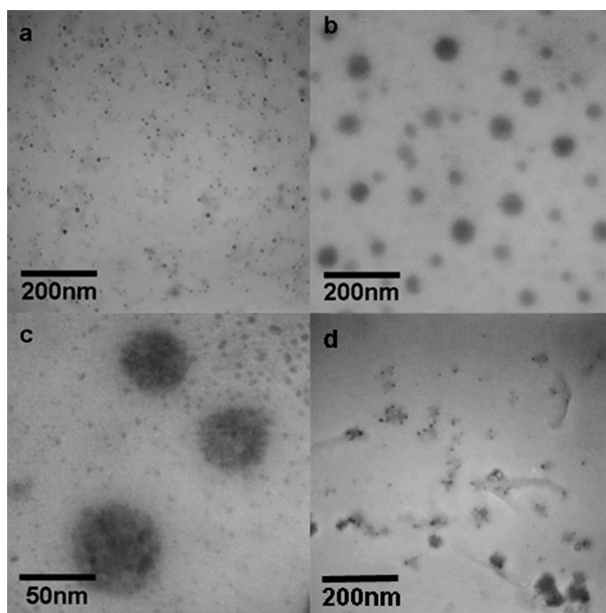


**Figure 4.** TEM images of self-assembled micelles obtained from 5 mg/mL POSS-PDMAEMA aqueous solution by varying the pH value from (a) pH 3.0 to (b) pH 9.0 and (c) a magnification of (b) and then back to (d) pH 3.0.

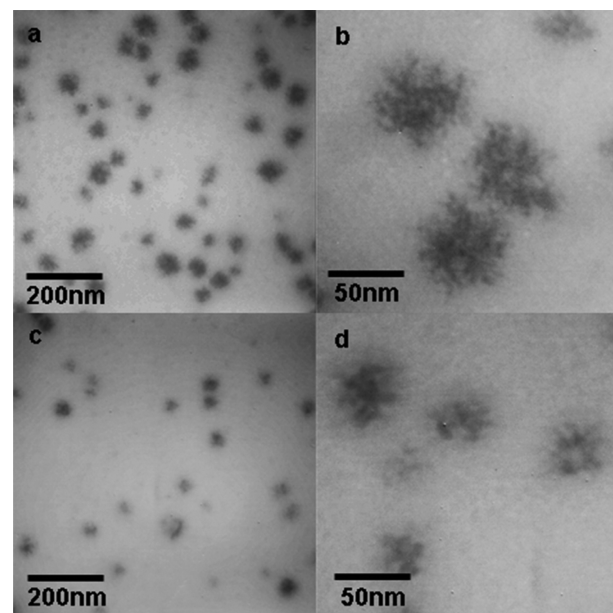


**Figure 5.** TEM images of self-assembled micelles obtained by adding (a) 70 and (c) 140  $\mu$ L of 1 M NaCl in 2 mL of POSS-PDMAEMA aqueous solution. (b) and (d) are magnifications of (a) and (c), respectively. The concentration of aqueous solution is 5 mg/mL.

**Table 1. Hydrodynamic Diameter and Size Polydispersity of Single and Complex Micelles**

	hydrodynamic diameter (nm)	size PDI
pH 3	79	0.29
pH 9	164	0.81
pH 3 <sup>a</sup>	86	0.3
salt 1	192	0.29
salt 2 <sup>b</sup>	107	0.22

<sup>a</sup> The pH value was adjusted from 9 back to 3. <sup>b</sup> The salt concentration of salt 2 was 2 times higher than that of salt 1.

Table 1, the hydrodynamic diameter of the micelle increased from 79 nm at pH 3 to 164 nm at pH 9 and then decreased to 86 nm when the pH value was adjusted back to 3. This trend proved the reversible change of the aggregate structure between the single micelle and the complex micelle.

We proposed a schematic illustration for the self-assembly process of POSS-PDMAEMA when the pH value of the aqueous solution varied, as shown in Scheme 2a. When the concentration of POSS-PDMAEMA aqueous solution is above the cmc value, POSS-PDMAEMA, driven by the POSS head, starts to aggregate into single micelles with POSS heads as the core and PDMAEMA chains as the corona (Scheme 2A). However, the PDMAEMA chains are not fully extended without the solution adjusted by acid, so the curly polymer chains prevent the micelles from becoming large. When the pH value of POSS-PDMAEMA aqueous solution decreases to 3, the PDMAEMA chains fully protonize and extend in the solution; therefore, micelles in Scheme 2D can form. Then, when the pH value is increased to 9, single micelles form a complex micelle-on-micelle structure (Scheme 2E). By varying the pH value, the micelle structure of POSS-PDMAEMA can be reversibly changed

between the single micelles in Scheme 2D and the complex micelles in Scheme 2E.

Also, salt was able to induce the single micelles to form the micelle-on-micelle structure. Ionic strength plays an important role in the self-assembly behavior because ions can screen the charge of the PDMAEMA chains and induce the aggregation of the single micelles. As shown in Figure 5a, flowerlike micelles are observed by adding NaCl into the polymer aqueous solution, and the aggregates with the size of ca. 20–65 nm are well-dispersed. When the ionic strength increases, the size of the complex micelles becomes small; as shown in Figure 5c, the size of the aggregates is ca. 15–50 nm. This trend is also proved by DLS measurements, as shown in Table 1. Because the ions decreased the electrostatic repulsion between the polymer chains, the size of the micelles became smaller at higher ionic strength. Scheme 2b illustrates how the ionic strength influences the self-assembly structure of POSS-PDMAEMA.

Temperature can also influence the self-assembly behaviors of POSS-PDMAEMA because the PDMAEMA chains can form hydrogen bonding with water molecules, and the hydrogen bonding will be broken when the temperature increases. The break of hydrogen bonding decreases the hydrophilicity of PDMAEMA chains and induces the aggregation of the single micelles. The transmittance of POSS-PDMAEMA aqueous solution decreases when the temperature increases (Figure S3 in the Supporting Information), which indicates that large aggregates formed at high temperature.<sup>38</sup>

## CONCLUSION

In conclusion, POSS-PDMAEMA was successfully synthesized via ATRP. The polymer can self-assemble into a hierarchical structure. When the concentration of the polymer aqueous solution was above the cmc value, POSS drove the polymers to self-assemble into the single micelles with the POSS heads

forming a crystal core and the PDMAEMA chains stretching as a corona. Then, under external stimuli, the single micelles, as building blocks, further aggregated into a reversible complex micelle-on-micelle structure.

## ■ ASSOCIATED CONTENT

**S Supporting Information.** FT-IR spectra of POSS–Br and POSS–PDMAEMA,  $^1\text{H}$  NMR spectrum of POSS–PDMAEMA, and effect of temperature on the transmittance of POSS–PDMAEMA aqueous solution. This material is available free of charge via the Internet at <http://pubs.acs.org>.

## ■ AUTHOR INFORMATION

### Corresponding Author

\*Phone/Fax: 86-10-64421693. E-mail: qflee@mail.buct.edu.cn.

## ■ ACKNOWLEDGMENT

The authors are thankful for financial support from the National Natural Science Foundation of China (No. 20974013), Polymer Chemistry and Physics, Beijing Municipal Education Commission (BMEC, No. XK100100640), and the Program for Changjiang Scholars and Innovative Research Team in University (PCSIRT, IRT0807).

## ■ REFERENCES

- (1) Liu, F.; Urban, M. W. *Prog. Polym. Sci.* **2010**, *35*, 3–23.
- (2) Motornov, M.; Roiter, Y.; Tokarev, I.; Minko, S. *Prog. Polym. Sci.* **2010**, *35*, 174–211.
- (3) Roy, D.; Cambre, J. N.; Sumerlin, B. S. *Prog. Polym. Sci.* **2010**, *35*, 278–301.
- (4) Hu, J. M.; Liu, S. Y. *Macromolecules* **2010**, *43*, 8315–8330.
- (5) Cayre, O. J.; Chagneux, N.; Biggs, S. *Soft Matter* **2011**, *7*, 2211–2234.
- (6) Ge, Z. S.; Liu, S. Y. *Macromol. Rapid Commun.* **2009**, *30*, 1523–1532.
- (7) Wan, X. J.; Liu, T.; Liu, S. Y. *Biomacromolecules* **2011**, *12*, 1146–1154.
- (8) Jiang, J. Q.; Tong, X.; Zhao, Y. *J. Am. Chem. Soc.* **2005**, *127*, 8290–8291.
- (9) Lee, H.; Wu, W.; Oh, J. K.; Mueller, L.; Sherwood, G.; Peteanu, L.; Kowalewski, T.; Matyjaszewski, K. *Angew. Chem., Int. Ed.* **2007**, *46*, 2453–2457.
- (10) Xu, J.; Liu, S. Y. *Soft Matter* **2008**, *4*, 1745–1749.
- (11) Mya, K. Y.; Li, X.; Chen, L.; Ni, X. P.; Li, J.; He, C. B. *J. Phys. Chem. B* **2005**, *109*, 9455–9462.
- (12) Hussain, H.; Tan, B. H.; Seah, G. L.; Liu, Y.; He, C. B.; Davis, T. P. *Langmuir* **2010**, *26*, 11763–11773.
- (13) Tan, B. H.; Hussain, H.; He, C. B. *Macromolecules* **2011**, *44*, 622–631.
- (14) Wei, J.; Tan, B. H.; Bai, Y.; Ma, J.; Lu, X. H. *J. Phys. Chem. B* **2011**, *115*, 1929–1935.
- (15) Loh, X. J.; Zhang, Z. X.; Mya, K. Y.; Wu, Y. L.; He, C. B.; Li, J. *J. Mater. Chem.* **2010**, *20*, 10634–10642.
- (16) Zhang, W. A.; Fang, B.; Walther, A.; Müller, A. H. E. *Macromolecules* **2009**, *42*, 2563–2569.
- (17) Zhang, W. A.; Liu, L.; Zhuang, X. D.; Li, X. H.; Bai, J. R.; Chen, Y. *J. Polym. Sci., Part A: Polym. Chem.* **2008**, *46*, 7049–7061.
- (18) Yu, X. F.; Zhong, S.; Li, X. P.; Tu, Y. F.; Yang, S. G.; Van Horn, R. M.; Ni, C. Y.; Pochan, D. J.; Quirk, R. P.; Wesdemiotis, C.; et al. *J. Am. Chem. Soc.* **2010**, *132*, 16741–16744.
- (19) Zhang, W. B.; Li, Y. W.; Li, X. P.; Dong, X. H.; Yu, X. F.; Wang, C. L.; Wesdemiotis, C.; Quirk, R. P.; Cheng, S. Z. D. *Macromolecules* **2011**, *44*, 2589–2596.
- (20) Zeng, K.; Fang, Y.; Zheng, S. X. *J. Polym. Sci., Part B: Polym. Phys.* **2009**, *47*, 504–516.
- (21) Liu, F.; Urban, M. W. *Macromolecules* **2008**, *41*, 6531–6539.
- (22) Yamamoto, S.; Pietrasik, J.; Matyjaszewski, K. *Macromolecules* **2008**, *41*, 7013–7020.
- (23) Tan, B. H.; Gudipati, C. S.; Hussain, H.; He, C. B.; Liu, Y.; Davis, T. P. *Macromol. Rapid Commun.* **2009**, *30*, 1002–1008.
- (24) Zhang, H.; Ni, P. H.; He, J. L.; Liu, C. C. *Langmuir* **2008**, *24*, 4647–4654.
- (25) Liu, Y. H.; Cao, X. H.; Luo, M. B.; Le, Z. G.; Xu, W. Y. *J. Colloid Interface Sci.* **2009**, *329*, 244–252.
- (26) Yu, H.; Gan, L. H.; Hu, X.; Gan, Y. Y. *Polymer* **2007**, *48*, 2312–2321.
- (27) Jiang, X. Z.; Ge, Z. S.; Xu, J.; Liu, H.; Liu, S. Y. *Biomacromolecules* **2007**, *8*, 3184–3192.
- (28) Petrov, P.; Tsvetanov, C. B. *J. Phys. Chem. B* **2009**, *113*, 7527–7533.
- (29) Kim, B. S.; Gao, H. F.; Argun, A. A.; Matyjaszewski, K.; Hammond, P. T. *Macromolecules* **2009**, *42*, 368–375.
- (30) Sui, K. Y.; Shan, X.; Gao, S.; Xia, Y. Z.; Zheng, Q.; Xie, D. *J. Polym. Sci., Part A: Polym. Chem.* **2010**, *48*, 2143–2153.
- (31) Bao, H. Q.; Hu, J. H.; Gan, L. H.; Li, L. *J. Polym. Sci., Part A: Polym. Chem.* **2009**, *47*, 6682–6692.
- (32) Liu, J. W.; Li, J. X.; Xie, M. R.; Ding, L.; Yang, D.; Zhang, L. Y. *Polymer* **2009**, *50*, 5228–5235.
- (33) Bougard, F.; Jeusette, M.; Mespoille, L.; Dubois, P.; Lazzaroni, R. *Langmuir* **2007**, *23*, 2339–2345.
- (34) Sin, S. L.; Gan, L. H.; Hu, X.; Tam, K. C.; Gan, Y. Y. *Macromolecules* **2005**, *38*, 3943–3948.
- (35) Yao, Z. L.; Tam, K. C. *Langmuir* **2011**, *27*, 6668–6673.
- (36) Matter, Y.; Enea, R.; Casse, O.; Lee, C. C.; Baryza, J.; Meier, W. *Macromol. Chem. Phys.* **2011**, *212*, 937–949.
- (37) Guo, S. T.; Wang, W. W.; Deng, L. D.; Xing, J. F.; Dong, A. J. *Macromol. Chem. Phys.* **2010**, *211*, 1572–1578.
- (38) Ma, L.; Liu, R. G.; Tan, J. J.; Wang, D. Q.; Jin, X.; Kang, H. L.; Wu, M.; Huang, Y. *Langmuir* **2010**, *26*, 8697–8703.
- (39) Liu, X.; Ni, P. H.; He, J. L.; Zhang, M. Z. *Macromolecules* **2010**, *43*, 4771–4781.
- (40) Guo, S. T.; Huang, Y. Y.; Wei, T.; Zhang, W. D.; Wang, W. W.; Lin, D. S.; Zhang, X.; Kumar, A.; Du, Q.; Xing, J. F.; et al. *Biomaterials* **2011**, *32*, 879–889.
- (41) Kalyanasundaram, K.; Thomas, J. K. *J. Am. Chem. Soc.* **1977**, *99*, 2039–2044.
- (42) Lodge, T. P.; Rasdal, A.; Li, Z. B.; Hillmyer, M. A. *J. Am. Chem. Soc.* **2005**, *127*, 17608–17609.
- (43) Li, Z. B.; Kesselman, E.; Talmon, Y.; Hillmyer, M. A.; Lodge, T. P. *Science* **2004**, *306*, 98–101.